T-wave Peak-to-End Changes Quantified by Time-Warping Predicts Ventricular Fibrillation in a Porcine Myocardial Infarction Model

Neurys Gómez, Julia Ramírez, Alba Martín-Yebra, Marina M. Demidova, Pyotr Platonov, Juan Pablo Martínez, and Pablo Laguna, *Fellow, IEEE*

Abstract*—*Background: **The T-peak-to-T-end (T_{pe}) interval has shown potential in predicting ventricular arrhythmic risk. It is an appealing index to be measured during ischemia since it is less influenced by ST-segment changes than the early part of the T wave. A time-warping-based index, derived from a spatially transformed PCA lead, $d^{\mathbf{PCA}}_{w,\mathrm{T}_{pe}}$, quantifying changes in the T_{pe} morphology, has previously demonstrated utility in tracking repolarization changes induced by a 5-minute ischemia model in humans. The value of $d^{\mathbf{PCA}}_{w,\mathrm{T}_{pe}}$ as a predictor of ventricular fibrillation (VF) episodes is assessed in a porcine model of myocardial ischemia with ischemia maintained for 40 minutes.** ***Methods:*** **From 32 pigs undergoing a coronary occlusion, pre-occlusion and occlusion ECG recordings from 10 pigs suffering a VF episode after 10 min of occlusion (Delayed VF) and 16 that did not had any episode during the recording were analyzed. The $d^{\mathbf{PCA}}_{w,\mathrm{T}_{pe}}$ series was measured by comparing T_{pe} morphologies at different stages of the occlusion relative to the peak-to-end morphology of a baseline T-wave.** ***Results:*** **During baseline, $d^{\mathbf{PCA}}_{w,\mathrm{T}_{pe}}$ remained stationary with an intra-recording median [IQR] value of 1.60 [1.33] ms. During artery occlusion, $d^{\mathbf{PCA}}_{w,\mathrm{T}_{pe}}$ followed a well-marked gradual increasing trend as ischemia progressed, reaching a median of 14.58 [17.72] ms. $d^{\mathbf{PCA}}_{w,\mathrm{T}_{pe}}$ averages were significantly higher ($p < 0.05$) in the VF group than in the Non-VF group at time intervals 0-5, 5-10, 10-15, 15-20, 20-25 min after occlusion onset and at 10-15, 5-10 and 5-0 minutes prior to VF episode, with median values of 12.5, 18.8, 26.8, 24.0, 31.0, 18.6, 25.0 and 28.8 vs 6.3, 7.6, 8.0, 7.8, 7.8, 8.5, 7.2 and 6.0 ms, respectively. The $\mathrm{T}^{\mathbf{PCA}}_{pe}$ interval was also significantly higher in the VF group at all analyzed time periods, but with a lower significance level. Pigs with maximum $d^{\mathbf{PCA}}_{w,\mathrm{T}_{pe}} \geq 20.0$ ms and $\mathrm{T}^{\mathbf{PCA}}_{pe} \geq 85.4$ ms had significantly higher risk for VF occurring in the early 5-10 minutes interval, with 90.0%/75.0% and 80.0%/69.0% sensitivity/specificity, respectively. Univariate Cox analysis yielded hazard ratios of 12.5 for $d^{\mathbf{PCA}}_{w,\mathrm{T}_{pe}}$ vs 5.5 for $\mathrm{T}^{\mathbf{PCA}}_{pe}$.** ***Conclusions and Significance:*** **The time-warping-based index, $d^{\mathbf{PCA}}_{w,\mathrm{T}_{pe}}$, is a stronger VF predictor than $\mathrm{T}^{\mathbf{PCA}}_{pe}$ during ischemia in a porcine model, advising for further clinical exploration studies in humans.**

***Index Terms*—Electrocardiogram, time warping, T-wave morphology, T-peak to T-end interval, ischemia, repolarization, ventricular arrhythmias.**

This paper was submitted for review on March 4, 2024. *Asterisk indicates corresponding author.*

N. Gómez* is with BSICoS group, I3A, IIS Aragón, University of Zaragoza, Zaragoza, Spain, and University of Oriente, Cuba (correspondence e-mail: ngomez@unizar.es).

J. Ramírez is with BSICoS group, I3A, IIS Aragón, University of Zaragoza, Zaragoza, Spain, with CIBER-BBN, Spain, and with William Harvey Research Institute, Queen Mary University of London, United Kingdom.

P. Platonov and M.M. Demidova are with Department of Cardiology, Clinical Sciences, Lund University, Lund, Sweden.

A. Martín, J. P. Martínez, and P. Laguna are with BSICoS group, I3A, IIS Aragón, University of Zaragoza, Zaragoza, and with CIBER-BBN, Spain.

I. Introduction

The development of life-threatening arrhythmias, such as ventricular fibrillation (VF), is the main cause of sudden cardiac death (SCD), in both myocardial infarction settings and the general population, remaining the leading cause of death worldwide [1], [2]. Thus, early prediction remain crucial for the implementation of prevention strategies. The link between ventricular repolarization alterations and the development of an arrhythmogenic substrate has been demonstrated both in experimental models and in clinical studies [3], [4], resulting in the identification of risk indicators that are, along with other relevant clinical information, suitable for risk stratification in the routine patient management.

Several T-wave indices have been studied to quantify the increase in ventricular repolarization dispersion (VRD) and predict ventricular arrhythmia [5]. Examples are T-wave alternans [6], [7], T-wave area dispersion [3], T wave morphology restitution (TMR) [8] and T-wave morphology variations [9], which are reported to be superior than traditional ECG indices in predicting arrhythmias. However, these biomarkers can also be influenced by other effects unrelated to the underlying electrical arrhythmogenic substrate. This occurs in ischemia, eventually concurring with ST elevation/depression and early T wave area affections, related to the ischemic injury currents, but not necessarily connected to the increased arrhythmic risk. Indices that make use of the whole T wave, like TMR or TMV, might, thus, become unsuitable for ischemia-related SCD risk stratification, motivating the investigation of alternative indices able to capture the specific information related to ventricular arrhythmia risk.

The T_{pe} interval was introduced as a surrogate measure of VRD in [10] and as a potential predictive index for arrhythmic risk in [11], [12]. Its potential to stratify arrhythmic risk has been evaluated using an arterially perfused canine ventricular wedge [10], where it was proposed as a measure of transmural dispersion of repolarization, although there is not yet a definite consensus as to whether it reflects transmural, apico-basal or a combination of the two types of dispersion [11], [13], [14]. In the past years, the T_{pe} interval has been extensively reported to be a predictive index of arrhythmic risk in different settings, such as long [15] and short [16] QT syndrome, vasospastic angina [17] and Brugada syndrome [18]. More recently, Azarov *et al.*[19] demonstrated the relationship between the evolution of the T_{pe} index and the development of

an arrhythmogenic substrate in a porcine myocardial infarction model.

Nevertheless, T_{pe} interval only quantifies a temporal difference between the end and the peak of the T-wave, hence the information contained within the morphology is not considered. To overcome these restrictions, the warping-based d_w index proposed by Ramírez *et al.* [8] was adapted to exclusively quantify morphological variations within the T_{pe} interval, demonstrating a great ability in quantifying ischemia-induced VRD changes in a 5-min ischemia model in humans [20]. However, the time span was not large enough to evaluate its potential for arrhythmia risk prediction. A previous work in an animal model of ischemia showed a promising VF classification potential of this T_{pe}-restricted d_w index [21], but its predictive value remains unknown.

The aim of this work was to analyze the time-course of the T_{pe} warping-based d_w VRD index during ischemia progression and to test whether its evolution could predict impending VF in a porcine myocardial infarction model.

II. Materials and Methods

A. Experimental Data Set and Protocol

This study uses a closed-chest porcine myocardial infarction model implemented at Lund University (Lund, Sweden). A detailed description of the experimental protocol can be found in [22]. Myocardial ischemia and infarction was induced by a 40-minute-long balloon inflation in the left anterior descending coronary artery (LAD) in 32 pigs. A 12-lead ECG with a sampling rate of 1024 Hz and amplitude resolution of 1.18 μV per bit was recorded at baseline and during coronary occlusion period using "Kardiotechnica-04-8", INCART, St.Petersburg, Russia.

The animal research study followed the guidelines in the Care and Use of Laboratory Animals guide by the US National Institutes of Health (NIH Publication No. 85-23, revised 1996) and received approval from the local animal research ethics committee.

TABLE I: Pig population and VF distribution.

Group	Pigs	Subgroup	Pigs	Occurrence time of VF event: mean [range] (min:s)
Non-VF	16	-	16	-
VF	16	Early VF	7	2:45 [0:49-7:3]
		Delayed-VF	10*	21:18 [17:40-30:50]

*one pig in the Delayed-VF group also suffered Early VF.

The pig population is divided as presented in Table I. From the total study group (32 pigs), 16 pigs did not have a VF event, while a total of 17 VF episodes were annotated in the remaining group. The VF group is further subdivided according to the VF occurrence time: a first subgroup (Early VF) is composed of 7 pigs suffering VF within the first 10 minutes of occlusion, and a second one (Delayed-VF), composed by the 10 pigs suffering VF after minute 10 from occlusion. One pig suffered VF twice, one in each of the defined periods. These two distinct subsets of VF are in line with the previously reported arrhythmic patterns [23], [24], where VF episodes were observed in two different periods of time, which are believed to have different underlying mechanisms. As early VF typically occur before patient's initial interaction with healthcare professionals, prediction of delayed-VF is more clinically relevant. Accordingly, this work focused on Delayed-VF occurring after the 10-th minute, and pigs who had early VF were excluded from the analysis as the VF prediction in human applications will not be technically feasible during the early minutes after occlusion.

B. ECG Pre-processing

First, the ECG was low-pass filtered for electric and muscle noise attenuation with a bidirectional sixth-order Butterworth filter with a 40-Hz cut-off frequency. Then, baseline wander was attenuated with a high-pass bidirectional sixth-order Butterworth filter with a 0.5 Hz cut-off frequency. Subsequently, a wavelet-based single-lead delineation method [25] was applied for ECG delineation at each of the eight independent leads to determine the QRS fiducial points. A unique set of multilead QRS fiducial points was obtained using a multilead selection rule strategy [26] applied over the 8 single-lead set of onsets and ends. This multilead delineation was used to determine the learning segment (T-wave segment) for the subsequent spatial transformation.

In this study, principal component analysis (PCA), used as a spatial transformation approach [27], was applied to the 8 independent ECG leads in order to emphasize the T-wave content, improving signal-to-noise ratio and facilitating accurate T-wave delineation. The transformed lead (i.e., the first principal component), assumed to be better suited for ECG delineation, was used for the subsequent ECG analysis.

The PCA eigenvectors and eigenvalues were estimated using the first minute of the baseline period, selecting T wave windows starting and ending at fixed distances from the corresponding QRS mark following the rules used in [28]. Finally, the first PCA transformed lead was delineated using the same single-lead technique [25]. The T wave was then segmented and further filtered (bidirectional Butterworth low-pass sixth-order filter with a 20-Hz cut-off frequency) to remove the remaining out-of-band high-frequency components.

C. Time-warping Quantification of T_{pe} Interval Changes

For each pig, ischemia-induced dynamic T peak-to-end waveform changes over time were quantified by both T_{pe} interval and by the time warping index d_w.

The d_w estimation follows the methodology proposed by Ramírez *et al.* in [8], with the adaptation proposed in [20] so that the calculation is restricted to the segment of the T wave between the T-peak and the T-end. Then, a mean warped T-peak-to-T-end wave (MWTPE), $\boldsymbol{f}^s(\boldsymbol{t}^s) = [f^s(t^s(1)), ..., f^s(t^s(N_s))]^T$ was estimated, where $\boldsymbol{t}^s = [t^s(1), ..., t^s(N_s))]^T$ contains the time samples of the MWTPE wave and $f^s(t)$ is the wave signal value at sample t, for each s-th moving signal window along the recording. In order to follow changes in this region of the T wave, a reference MWTPE, $\boldsymbol{f}^r(\boldsymbol{t}^r)$ was selected, and the temporal reparametrization (warping) was computed between each MWTPE along the recording and the reference. In brief, at

each recording, a MWTPE was extracted from each s-th 15-second sliding window (with 10-second overlap) over the entire record. The reference MWTPE was computed in a 60-second window at the beginning of the baseline stage, as shown in Fig. 1, where the d_w series estimation procedure is illustrated.

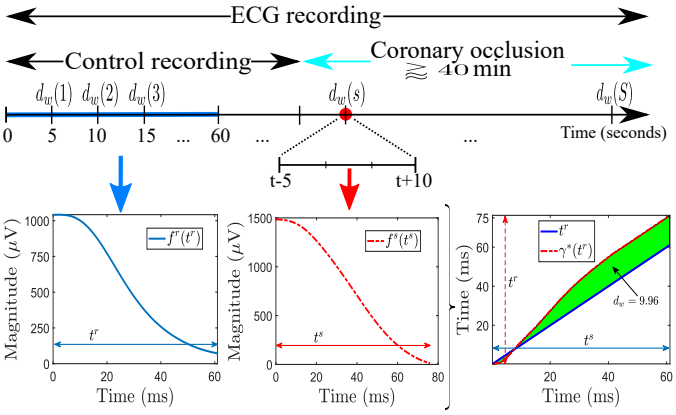

Fig. 1: Diagram of the method to obtain each MWTPE and the reference MWTPE and the d_w series. The MWTPE $\boldsymbol{f}^s(\boldsymbol{t}^s)$ was extracted from each s-th 15-second windows (represented by red color), with 5 seconds sliding and 10 seconds overlap the entire record, while MWTPE $\boldsymbol{f}^r(\boldsymbol{t}^r)$ was estimated from the waves within the first 60 seconds, at the beginning of the baseline period (blue color). The bottom rightmost graph shown the warping function $\gamma^*(t^r)$ (dotted red line) relating optimally the reference $\boldsymbol{f}^r(\boldsymbol{t}^r)$ and studied $\boldsymbol{f}^s(\boldsymbol{t}^s)$ MWTPEs. The green region between $\gamma^*(t^r)$ and t^r denotes the total warping amount, quantified by d_w.

Let $\gamma(\boldsymbol{t}^r)$ be the warping function that relates $\boldsymbol{t}^r$ and $\boldsymbol{t}^s$ such that the composition $[\boldsymbol{f}^s \circ \gamma](\boldsymbol{t}^r) = \boldsymbol{f}^s(\gamma(\boldsymbol{t}^r))$. That is, it denotes the time-warping or re-parameterization of the $\boldsymbol{f}^s(\boldsymbol{t}^s)$ using $\gamma(\boldsymbol{t}^r)$. As in [8], the square-root slope function (SRSF) was used to find the optimal warping function, avoiding any potential "pinching effect". The SRSF is calculated as the square-root of the derivative of $\boldsymbol{f}(\boldsymbol{t})$, considering the sign:

$$\boldsymbol{q}_f(\boldsymbol{t}) = sign\left(\dot{\boldsymbol{f}}(\boldsymbol{t})\right)\sqrt{|\dot{\boldsymbol{f}}(\boldsymbol{t})|}. \tag{1}$$

The optimal warping function, $\gamma^*(\boldsymbol{t}^r)$, is chosen as the one minimizing the amplitude difference between the SRSF of $\boldsymbol{f}^r(\boldsymbol{t}^r)$ and $\boldsymbol{f}^s(\gamma(\boldsymbol{t}^r))$ [29],

$$\begin{aligned}\gamma^*(\boldsymbol{t}^r) &= \underset{\gamma(\boldsymbol{t}^r)}{\arg\min}\left(\|\boldsymbol{q}_{f^r}(\boldsymbol{t}^r) - \boldsymbol{q}_{|f^s\circ\gamma|}(\boldsymbol{t}^r)\|\right) \\ &= \underset{\gamma(\boldsymbol{t}^r)}{\arg\min}\left(\|\boldsymbol{q}_{f^r}(\boldsymbol{t}^r) - \boldsymbol{q}_{f^s}(\gamma(\boldsymbol{t}^r))\sqrt{\dot{\gamma}(\boldsymbol{t}^r)}\|\right).\end{aligned} \tag{2}$$

The dynamic programming algorithm [30] was used to solve this optimization problem. The warping function $\gamma^*(\boldsymbol{t}^r)$, that optimally relates $\boldsymbol{f}^s(\boldsymbol{t}^s)$ and $\boldsymbol{f}^r(\boldsymbol{t}^r)$ (red and blue waves, respectively, at the bottom left panels of Fig. 1) is displayed at the bottom rightmost panel of the same Fig. 1.

The d_w index, quantifying the mean level of warping needed to optimally fit the two MWTPEs, is defined as:

$$d_w = \frac{1}{N_r}\sum_{n=1}^{N_r}|\gamma^*(\boldsymbol{t}_r(n)) - \boldsymbol{t}^r(n)|. \tag{3}$$

In order to test the impact of the first part of the T-wave (up to T-peak) in our hypothesis, we applied the same methodology to the whole T-wave. Since the T-wave onset (T_o) is strongly influenced by ischaemic conditions and, therefore, highly exposed to delineation errors, we chose the end of the QRS complex (QRS_e) to mark the beginning of the T-wave. When required, d_w will be denoted as $d^l_{w,\mathcal{I}}$, with l denoting the lead where the index is measured and $\mathcal{I} \in \{\mathrm{T}, \mathrm{T}_{pe}\}$ indicating the part of the T-wave where the measurement is taken.

The T_{pe} interval was also estimated to serve as a comparative reference to assess the added value of the $d^{\mathrm{PCA}}_{w,\mathrm{T}_{pe}}$. It was determined for each i-th beat as the difference between its T-end and T-peak time instants. A median filter was then applied to the resulting $\mathrm{T}^{\mathrm{PCA}}_{pe}$ series using a 15-second sliding window and 5 seconds of overlap to achieve the same resolution as that of the $d^{\mathrm{PCA}}_{w,\mathrm{T}_{pe}}$ index.

D. Statistical Analysis

The dynamic analysis of the ischemia-induced changes was performed by evaluating the time courses of $d^{\mathrm{PCA}}_{w,\mathrm{T}_{pe}}$, $\mathrm{T}^{\mathrm{PCA}}_{pe}$ and $d^{\mathrm{PCA}}_{w,\mathrm{T}}$ every 5 seconds in the baseline and the occlusion stages, presenting them as running averages and standard deviations. Average values during the first 5 minutes following recording onset (0-5), the last 5 minutes before the occlusion onset, the 0-5, 5-10, 10-15, 15-20, 20-25 five minutes intervals after occlusion, and during 15-10, 10-5 and 5-0 five minutes intervals, prior to a VF episode, were also computed, see Fig.3, top panel, for a schematic representation by arrows of the intervals. These values were compared between the group of VF-free pigs (Non-VF group) and those pigs who suffered Delayed-VF during coronary occlusion (Delayed-VF group). The Mann-Whitney test was used for comparisons between Non-VF and Delayed-VF groups. A p-value ≤ 0.05 was used to declare statistical significance.

To analyze the relationship between indices and VF-susceptibility, the maximum values into the above-mentioned periods were assessed. Receiver operating characteristic (ROC) curve analysis was used to find the true positive and false positive rate as the threshold varies. The optimal thesholds were taken as those that minimizes the distance to the upper left corner of the ROC curve. Then, the Cox regression analysis and Kaplan–Meier survival functions were used to comparatively analyze their predictor value. All computations were performed using MATLAB® version R2022a.

III. Results

A. Changes of $d^{PCA}_{w,\mathrm{T}_{pe}}$ During Occlusion

Fig. 2 shows, for a particular pig from the database, noticeable changes in the ECG beats and T_{pe} waveform during the occlusion, together with their projection on the first PCA transformed lead. Note that the greatest changes in the ECG

This article has been accepted for publication in IEEE Transactions on Biomedical Engineering. This is the author's version which has not been fully edited and content may change prior to final publication. Citation information: DOI 10.1109/TBME.2024.3404254

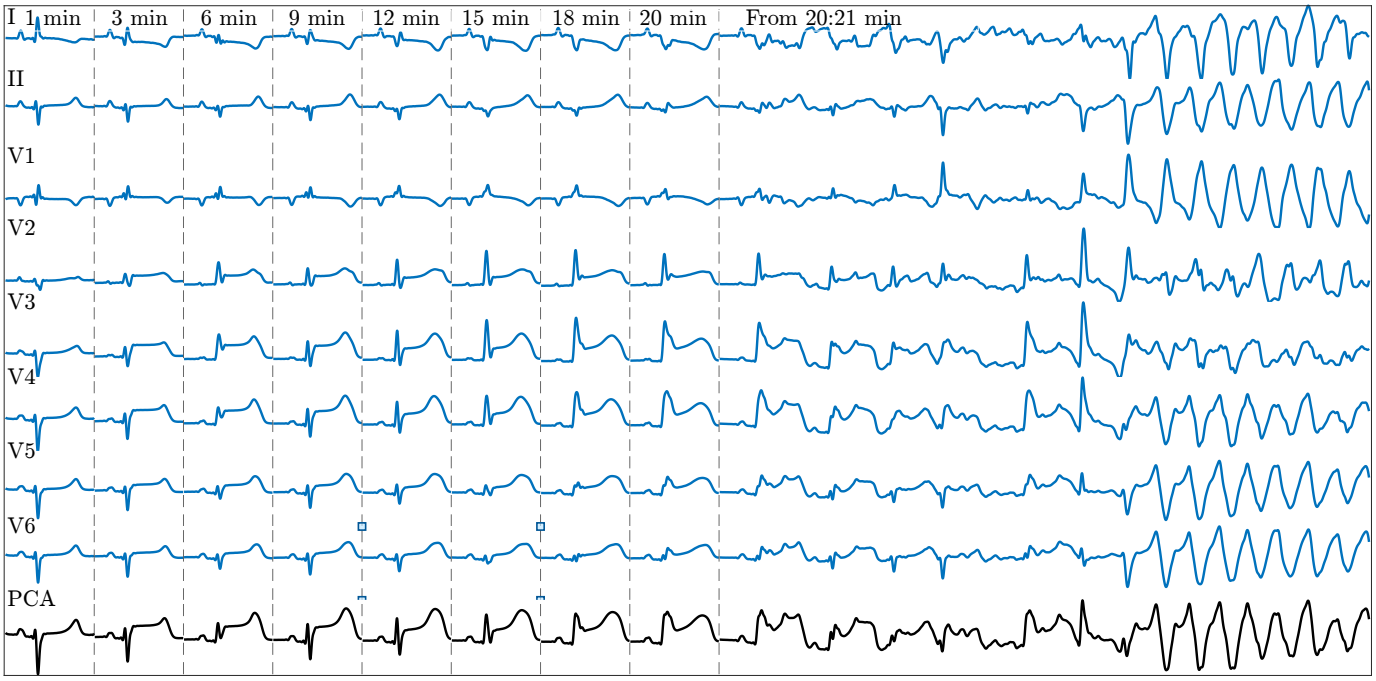

(a)

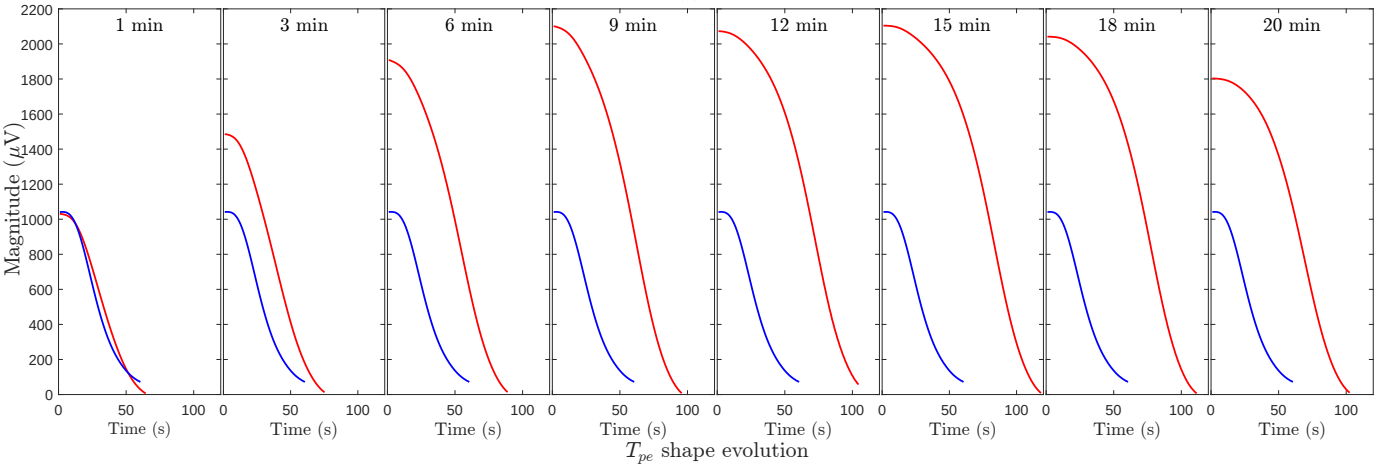

(b)

Fig. 2: Example of an ECG signal and T_{pe} interval waveform changes during coronary occlusion for a particular pig. Panel (a) shows representative QRST complexes recorded in 8 independent ECG leads and their projection on the first PCA transformed lead at 1, 3, 6, 9, 12, 15, 18, 20th and 21th minutes of LAD-occlusion, followed by ventricular fibrillation episode. Note that from the 20:21 min onwards the ECG beat shape is lost and the VF episode starts. Panel (b) shows the MWTPEs at the first PCA lead corresponding to each s-th window where ECG beat from panel (a) is contained, the blue line represents the reference $\boldsymbol{f}^r(\boldsymbol{t}^r)$ MWTPE and the red line each s-th given $\boldsymbol{f}^s(\boldsymbol{t}^s)$ MWTPE.

morphology appear on the leads most directly covering the LAD artery perfused area (V2-V4).

Changes in the T_{pe} waveform were captured by the $d^{\mathrm{PCA}}_{w,\mathrm{T}_{pe}}$ index, with an increasing trend beginning immediately after the start of the occlusion. An example of the time course of $d^{\mathrm{PCA}}_{w,\mathrm{T}_{pe}}(s)$ during baseline and occlusion for two particular animals, one who suffered VF and one who did not, is shown in Fig. 3. The dashed black line represents the balloon inflation instant and the dashed red lines indicate the occurrence of the VF episode. Strong intra-individual differences on the T_{pe} morphology variations in terms of $d^{\mathrm{PCA}}_{w,\mathrm{T}_{pe}}(s)$ magnitude changes were observed. These differences follow a more emphasized increasing trend as inflation time progresses for the pig who had VF than for the one that did not, ranging from 4.92 to 44.51 ms and from 1.94 to 7.52 ms, respectively, on the pigs in Fig. 3. In both baseline recordings, $d^{\mathrm{PCA}}_{w,\mathrm{T}_{pe}}(s)$ magnitude remains almost stationary, ranging from 0 to 8.67 and from 0 to 3.15 ms, respectively.

Across all the studied pigs, no significant T_{pe} morphology changes were found during baseline, with an inter-recordings median [IQR] value of the intra-recording median of 1.60 [1.33] ms. Six pigs showed a minor trend of change at the end

This article has been accepted for publication in IEEE Transactions on Biomedical Engineering. This is the author's version which has not been fully edited and content may change prior to final publication. Citation information: DOI 10.1109/TBME.2024.3404254

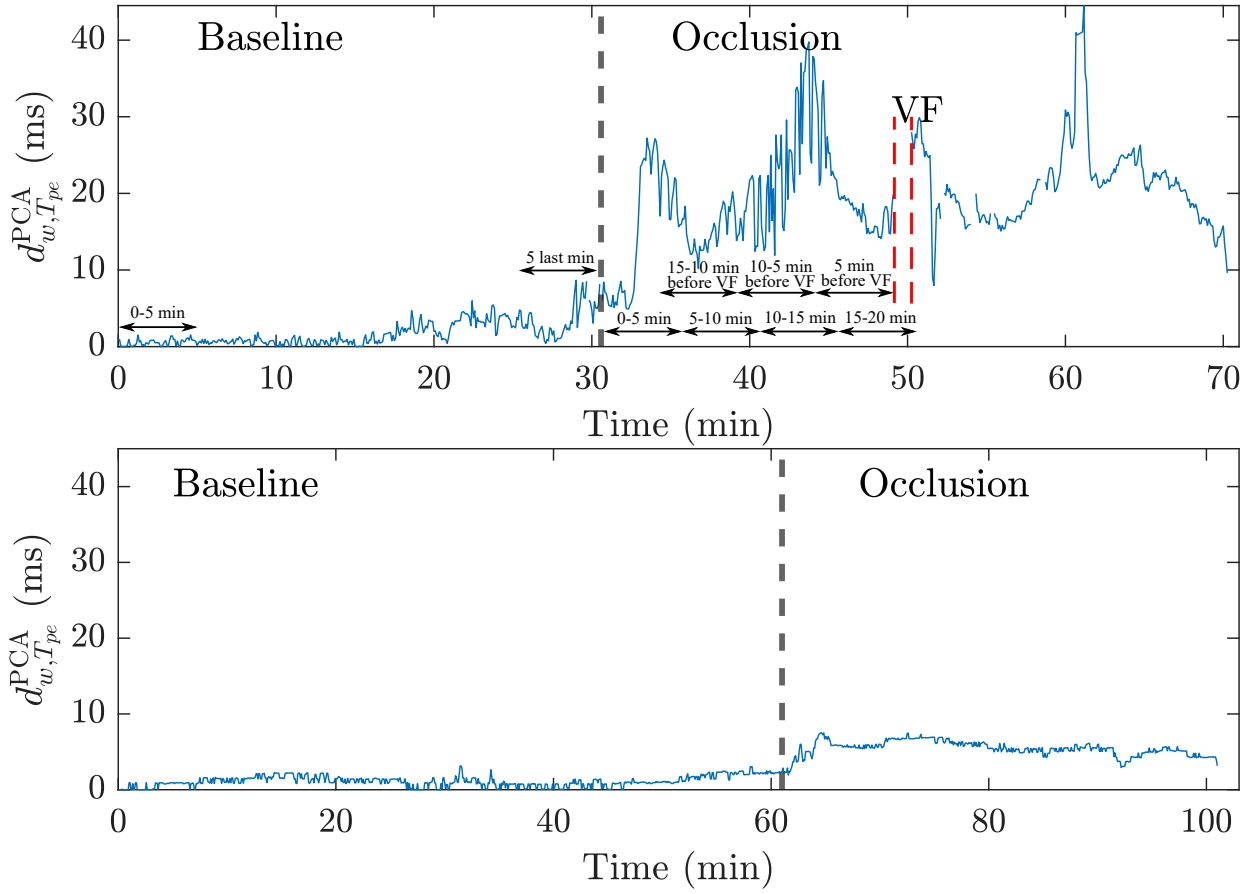

Fig. 3: Example of $d^{\text{PCA}}_{w,\text{T}_{pe}}(s)$ time course evolution along baseline and occlusion period for two particular animals, one who suffered a VF event (top) and one who did not (bottom). The black dashed line represents the onset of balloon inflation and the red dashed line, the occurrence of the VF episode.

of the control recording, as illustrated in Fig. 3, which may be due to catheter manipulations immediately before occlusion. In contrast, strong ischemia-induced changes, reflected in T_{pe} morphology changes (width and amplitude changes, together with the presence of T-wave alternans) and increased $d^{\text{PCA}}_{w,\text{T}_{pe}}$ magnitude were noted during the balloon inflation period in most of the pigs with intra-recording median values reaching 14.58 [17.72] ms.

B. Comparison of Indices Behaviour

The $d^{\text{PCA}}_{w,\text{T}_{pe}}$ and $\text{T}^{\text{PCA}}_{pe}$ indices showed similar behavior over time, characterized by an increase in their magnitudes from the beginning of the occlussion, with the greatest changes occurring in the first 5 minutes and remaining relatively stable thereafter. The average time course (blue line) and standard deviation (red line) of $d^{\text{PCA}}_{w,\text{T}_{pe}}$ and $\text{T}^{\text{PCA}}_{pe}$ indices across animals for the Non-VF and the Delayed-VF groups, both during baseline and occlusion stages, aligned to the recording onset or to the balloon inflation onset, respectively, are shown in Fig. 4. All recordings for each subset were averaged. Note that the number of available recordings declines as time elapses, at baseline due to the variable recording duration and at occlusion due to the different VF occurrence times.

The $d^{\text{PCA}}_{w,\text{T}_{pe}}$ and $\text{T}^{\text{PCA}}_{pe}$ indices exhibited similar behavior during baseline for the two groups of pigs, while $d^{\text{PCA}}_{w,\text{T}}$ showed a wider range of early changes but there were no significant differences between groups in the 5 minutes prior to the onset of balloon inflation. The average of $d^{\text{PCA}}_{w,\text{T}_{pe}}$, $\text{T}^{\text{PCA}}_{pe}$ and $d^{\text{PCA}}_{w,\text{T}}$ indices measured in the first 5 minutes after the baseline recording onset, at the last 5 minutes before the occlusion onset, at the 0-5, 5-10, 10-15, 15-20, 20-25 minutes from the occlusion onset and at the 15-10, 10-5 and 5 minutes prior to VF episode (or 21:18 min if no VF episode is present) are displayed in Fig. 5. The median magnitude for each interval and group and p-values of the comparison between groups (Mann-Whitney test) is shown in Table II. During occlusion, significant differences were found in the magnitude of the $d^{\text{PCA}}_{w,\text{T}_{pe}}$ and $\text{T}^{\text{PCA}}_{pe}$ indices when comparing VF-susceptible pigs (Delayed-VF group) and the Non-VF group from the first 5 minutes of balloon inflation, ranged from a negligible variation immediately before the onset of the occlusion to more pronounced differences as time elapses. Note that the p-value for $d^{\text{PCA}}_{w,\text{T}_{pe}}$ (0.037) during the first 5 minutes of ischemia is smaller than for $d^{\text{PCA}}_{w,\text{T}}$ (0.617), denoting superiority of $d^{\text{PCA}}_{w,\text{T}_{pe}}$ for early risk warning.

C. VF prediction analysis

The significantly greater increase of $d^{\text{PCA}}_{w,\text{T}_{pe}}$ and $\text{T}^{\text{PCA}}_{pe}$ magnitude as the duration of the occlusion progresses in the

This article has been accepted for publication in IEEE Transactions on Biomedical Engineering. This is the author's version which has not been fully edited and content may change prior to final publication. Citation information: DOI 10.1109/TBME.2024.3404254

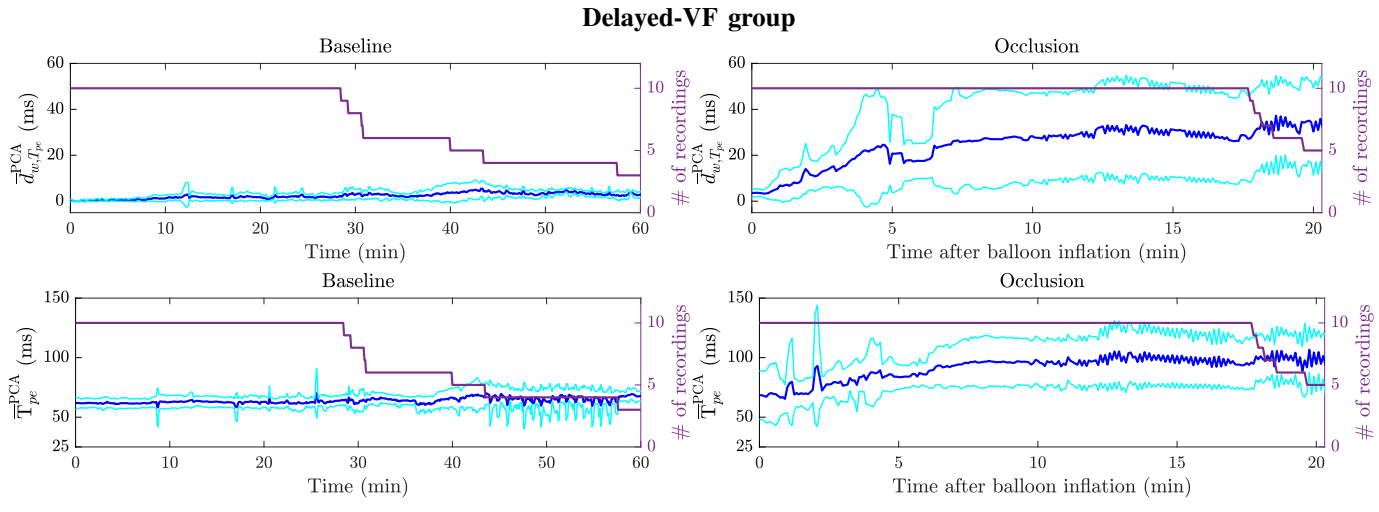

(a)

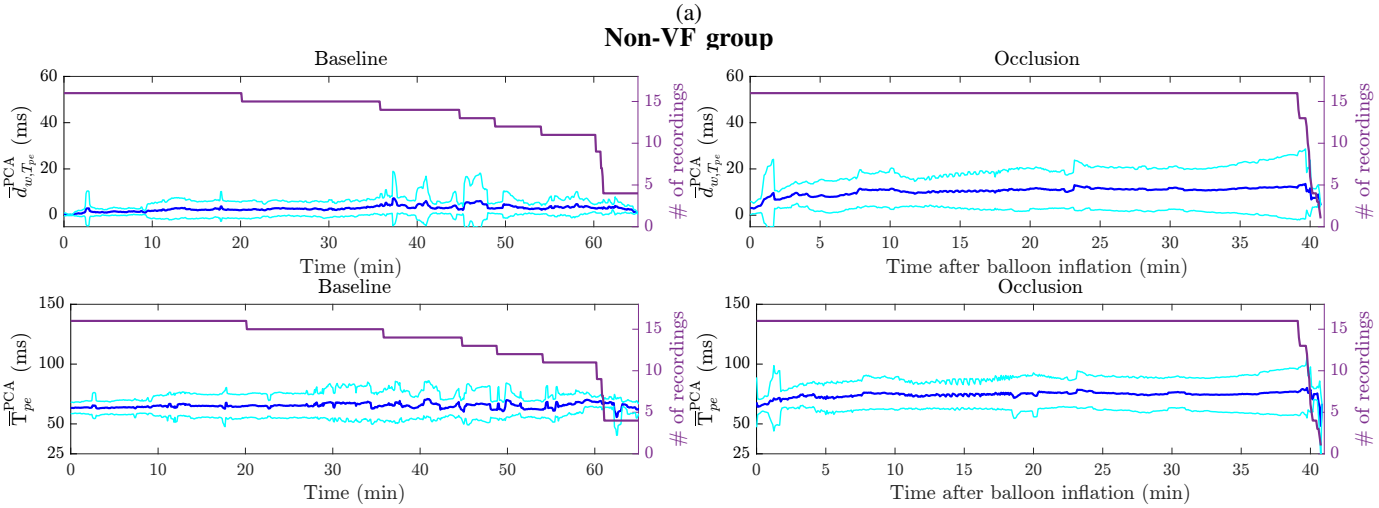

(b)

Fig. 4: Average time course of $d^{\text{PCA}}_{w,\text{T}_{pe}}$ and $\text{T}^{\text{PCA}}_{pe}$ indices (mean (blue line) $\pm$ standard deviation (cyan lines)) relative to the onset of the recording in baseline and to the balloon inflation onset during occlusion stage for pigs who suffered VF (Delayed-VF group) in panel (a) and for Non-VF group in panel (b). Purple line and the right y-axis indicate the number of averaged recordings at each given time. Note that the time span of the Delayed-VF and Non-VF groups are different for the occlusion stage due to the VF episodes occurrence. At baseline, the recording time is variable among pigs.

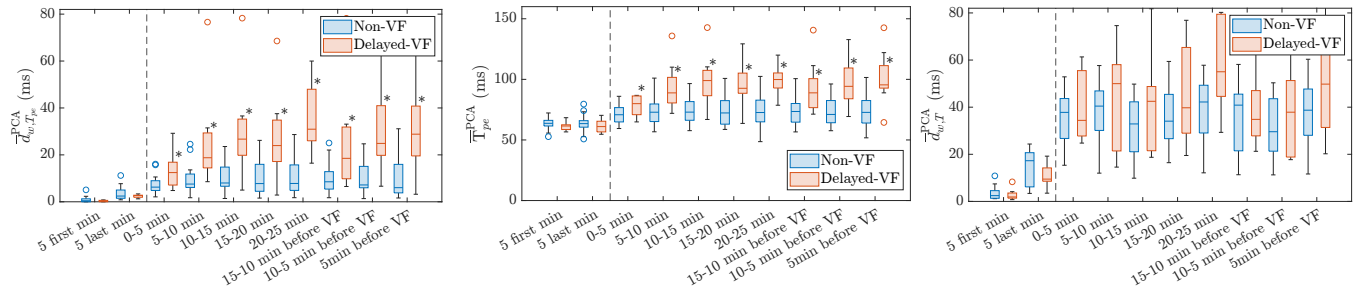

(a) (b) (c)

Fig. 5: Box plots distributions of $d^{\text{PCA}}_{w,\text{T}_{pe}}$ (a), $\text{T}^{\text{PCA}}_{pe}$ (b) and $d^{\text{PCA}}_{w,\text{T}}$ (c) for the Delayed-VF group (red) and Non-VF group (blue), measured in the first five minutes, 0-5, after the recording onset, at the last five minutes, 5-0, prior the occlusion onset, during occlusion recording at the 1-5, 5-10, 10-15, 15-20, 20-25 five minutes intervals and at the 15-10, 10-5 and 5-0 five minutes intervals prior to VF episode. The black dashed line represents the beginning of balloon inflation and * indicates statistical significance for comparison between groups.

TABLE II: Median and p-value from selected intervals for $d^{\text{PCA}}_{w,\text{T}_{pe}}$, $\text{T}^{\text{PCA}}_{pe}$ and $d^{\text{PCA}}_{w,\text{T}}$ indices segregated by VF susceptibility.

Index		Control stage		Occlusion stage							
		0-5 min onset	5-0 min before occl	0-5 min	5-10 min	10-15 min	15-20 min	20-25 min	15-10 min before VF	10-5 min before VF	5-0 min before VF
$d^{\text{PCA}}_{w,\text{T}_{pe}}$	Delayed-VF group median (s)	0.3	2.7	12.5	18.8	26.8	24.0	31.0	18.6	25.0	28.8
	Non-VF group median (s)	0.4	2.4	6.3	7.6	8.0	7.8	7.8	8.5	7.2	6.0
	p-value	0.340	0.843	0.037	0.001	0.001	0.008	0.003	0.016	0.002	0.004
$\text{T}^{\text{PCA}}_{pe}$	Delayed-VF group median (s)	61.5	61.0	80.0	89.0	99.0	92.6	99.0	88.9	94.2	95.5
	Non-VF group median (s)	63.7	63.5	70.8	72.9	73.0	72.3	72.6	73.5	71.0	72.8
	p-value	0.187	0.383	0.042	0.003	0.002	0.008	0.019	0.030	0.003	0.002
$d^{\text{PCA}}_{w,\text{T}}$	Delayed-VF group median (s)	1.9	9.5	34.4	50.0	42.5	39.7	55.0	34.8	37.9	49.8
	Non-VF group median (s)	2.5	17.3	37.8	40.5	32.9	34.1	42.2	40.9	29.6	38.7
	p-value	0.654	0.295	0.617	0.414	0.257	0.216	0.076	0.732	0.544	0.12

VF-susceptible pigs compared to the Non-VF pigs offered a rationale for assessing their values for predicting VF episodes. Therefore, the association between the maximum amplitude of both indices (together with that of the $d^{\text{PCA}}_{w,\text{T}}$ index as comparative reference) and the subsequent VF episode at the intervals 0-5, 5-10 minutes (first minutes of occlusion) and 5-0 minutes before the episode of VF, was studied using the receiver operating characteristic (ROC) curve, shown in Fig. 6 and completed in Table III. Results show improved detection ability for $d^{\text{PCA}}_{w,\text{T}_{pe}}$ (AUC=0.85) as compared with $\text{T}^{\text{PCA}}_{pe}$ (AUC=0.79) within the early 5-10 minutes interval. Taking the threshold that minimizes the distance to the upper left corner of the ROC curve, results show that $d^{\text{PCA}}_{w,\text{T}_{pe}}$ predicts the presence of VF episodes with Se=90%, Sp=75% for a threshold set to 20.0 ms, whereas the $\text{T}^{\text{PCA}}_{pe}$ index distinguishes between both groups with a lower accuracy (Se=80%, Sp=69% for a threshold set to 85.4 ms) and for $d^{\text{PCA}}_{w,\text{T}}$ index there was no significant association between the index magnitude and the delayed-VF occurrence. For the 1 to 5 minutes interval, lower values of AUC were obtained for $d^{\text{PCA}}_{w,\text{T}_{pe}}$, $\text{T}^{\text{PCA}}_{pe}$ and $d^{\text{PCA}}_{w,\text{T}}$ indices (AUC = 0.74, 0.66 and 0.60, respectively).

The presented analysis showed a significant association between both indices and the trigger of VF episodes at the time span prior to the arrhythmic window (more clinically relevant than the 5-minute interval before VF). The Cox regression analysis of $d^{\text{PCA}}_{w,\text{T}_{pe}} \geq 20.0$ predicted impending VF episodes with a hazard ratio of 12.5, whereas $\text{T}^{\text{PCA}}_{pe} \geq 85.4$ showed a hazard ratio of 5.5, see Table IV. The Kaplan–Meier survival functions for $d^{\text{PCA}}_{w,\text{T}_{pe}}$ and $\text{T}^{\text{PCA}}_{pe}$ indices are shown in Fig. 7. Significant differences in VF occurrence between the group of pigs with $d^{\text{PCA}}_{w,\text{T}_{pe}} \geq 20.0$ ms and the group with < 20.0 ms were obtained (Long Rank $p = 0.002$), whereas a $p = 0.016$ was obtained when the index $\text{T}^{\text{PCA}}_{pe}$ was used for classification.

IV. Discussion

The present study analyzes the behavior of the $d^{\text{PCA}}_{w,\text{T}_{pe}}$ index, restricted from the peak to the end of the T-wave, in a porcine model of prolonged ischemia, and assesses its VF predictive value as ischemia progresses. Changes in T_{pe} interval were measured using a time-warping-based morphological assessment methodology, characterizing its time course and comparing with the classical index, $\text{T}^{\text{PCA}}_{pe}$, and the original, complete T wave, d_w index denoted by $d^{\text{PCA}}_{w,\text{T}}$. Our main finding is that $d^{\text{PCA}}_{w,\text{T}_{pe}}$ predicts VF episodes more robustly and strongly than $\text{T}^{\text{PCA}}_{pe}$ index, whereas $d^{\text{PCA}}_{w,\text{T}}$ does not predict VF episodes.

A. Time-course of $d^{PCA}_{w,\text{T}_{pe}}$

The analysis of the time course of $d^{\text{PCA}}_{w,\text{T}_{pe}}$ confirmed, as in [20], the ability to reflect the ischemia-induced changes of repolarization dispersion through the monitoring of the morphological variations from the peak to the end of the T wave, avoiding early changes of the T wave under the ischemia-induced ST elevation/depression influence. We demonstrated that $d^{\text{PCA}}_{w,\text{T}_{pe}}$ showed a stationary behavior during baseline, while larger changes were observed during the 40-min of occlusion. As expected, the intra-recording median value for baseline oscillates in a narrow range while for the occlusion stage, the range is much wider (with median and IQR value 13 times larger than those obtained at baseline). The low values at baseline (non-ischemia conditions) indicate a stable $d^{\text{PCA}}_{w,\text{T}_{pe}}$ behavior, reflecting just natural ECG beat-to-beat variability.

From the occlusion onset, strong ischemic-induced changes were verified at the T_{pe} waveform, reflected by a well-marked increase trend of the $d^{\text{PCA}}_{w,\text{T}_{pe}}$ magnitude as the exposure time to ischemia elapses. The changes were greater for the VF-susceptible pigs group than for the pigs who did not suffer VF (see Fig. 3 and 4). It is likely that this marked increase are related to the differential shortening of the repolarization time of the action potential in the ischemic myocardium. These findings are in line with those reported in [19], where they described a marked T_{pe} increase during coronary occlusion as a consequence of the shortening of the Q-to-Tpeak interval, QTc_{peak}, together with moderate changes in the Q-to-Tend interval, QTc, along the whole recording.

The spatial lead-wise profile of $d^{\text{L}}_{w,\text{T}_{pe}}$, L$\in$\{V1,...,V6, aVL, I, aVR, II, aVF, III\}, analyzed under ischemia showed distinct distributions depending on the occluded artery [20], suggesting a relation with the ischemia location, although the differences in lead profile were not strong. Moreover, there is a gain in delineation robustness when PCA-transformed lead is used. Additionally, this study does not include occlusions in arteries other than LAD, mitigating the possible lead-dependency of results, limited to inter-individual artery tree configuration variability. We have therefore decided to analyze a unique time-warping based index computed from the global PCA-transformed lead instead of from specific leads.

B. Association with VF episodes

Both $d^{\text{PCA}}_{w,\text{T}_{pe}}$ and $\text{T}^{\text{PCA}}_{pe}$ indices presented an increasing trend as ischemia progressed. The greatest changes occurred in the first 5 minutes from the beginning of the coronary occlusion,

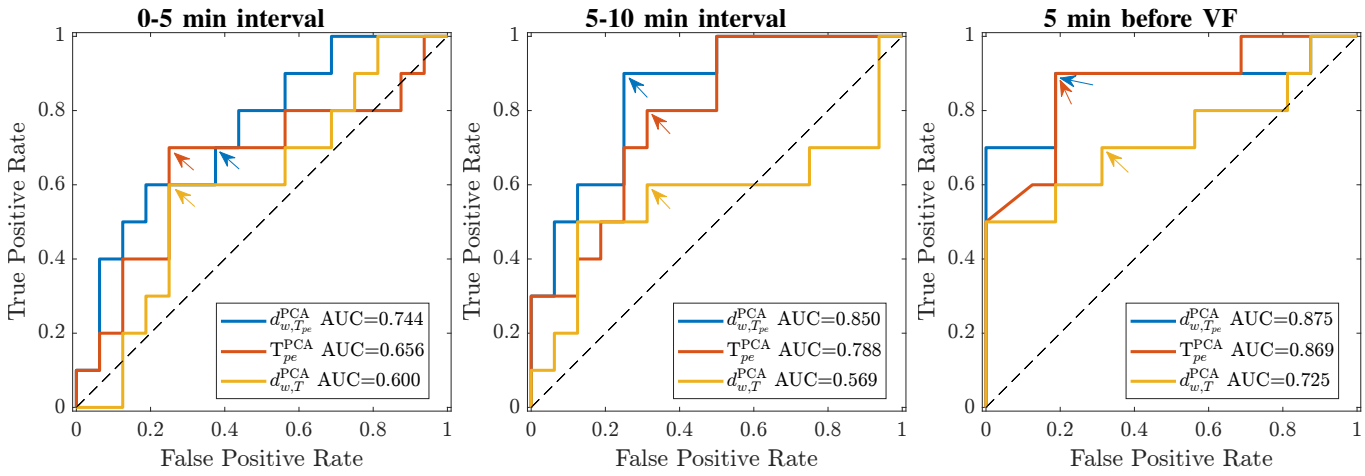

(a) (b) (c)

Fig. 6: Identification of the optimal $d^{\mathrm{PCA}}_{w,\mathrm{T}_{pe}}$, $\mathrm{T}^{\mathrm{PCA}}_{pe}$ and $d^{\mathrm{PCA}}_{w,\mathrm{T}}$ cut-off values to predict VF during the occlusion. The receiver operating characteristic (ROC) curve for three intervals: 0-5 minutes (panel (a)) and 5-10 five minutes intervals (panel (b)) after beginning of the occlusion and 5-0 five minutes interval prior to VF episode (panel (c)), are presented. The value of the area under the curve (AUC) is reported at the inside of the panels and the location on the ROC of the optimal thresholds have been marked using color coded arrows.

TABLE III: Threshold values together with sensibility and specificity values for VF prediction, and the AUC for $d^{\mathrm{PCA}}_{w,\mathrm{T}_{pe}}$, $\mathrm{T}^{\mathrm{PCA}}_{pe}$ and $d^{\mathrm{PCA}}_{w,\mathrm{T}}$ indices, calculated at three different time intervals.

	$d^{\mathrm{PCA}}_{w,\mathrm{T}_{pe}}$				$\mathrm{T}^{\mathrm{PCA}}_{pe}$				$d^{\mathrm{PCA}}_{w,\mathrm{T}}$			
Intervals	Thresholds (ms)	Se (%)	Sp (%)	AUC	Thresholds (ms)	Se (%)	Sp (%)	AUC	Thresholds (ms)	Se (%)	Sp (%)	AUC
1-5 min	13.4	70.0	62.5	0.74	83.0	70.0	75.0	0.66	67.6	60.0	75.0	0.60
5-10 min	20.0	90.0	75.0	0.85	85.4	80.0	69.0	0.79	57.9	60.0	68.8	0.57
5-0 before VF	22.0	90.0	81.3	0.88	94.7	90.0	81.3	0.87	60.0	70.0	68.8	0.73

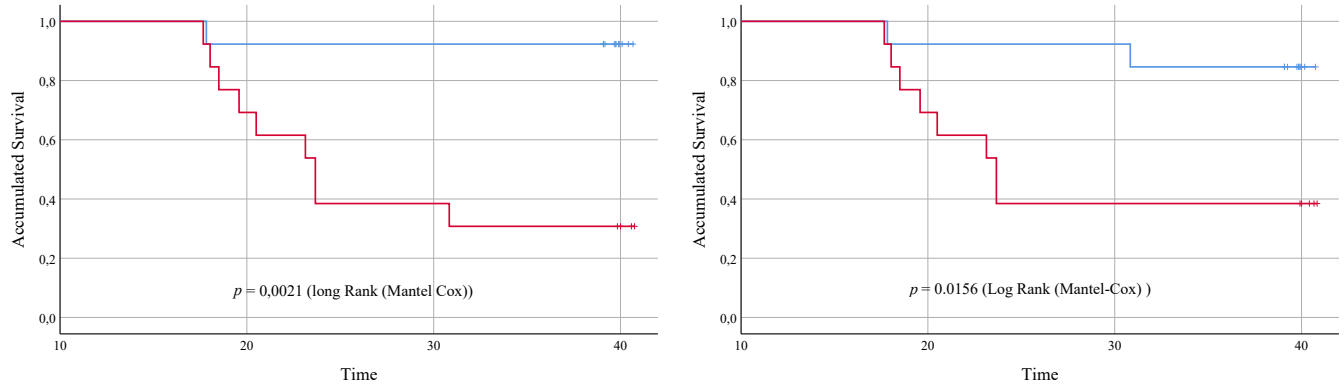

(a) (b)

Fig. 7: Kaplan–Meier survival curves for the pigs with $d^{\mathrm{PCA}}_{w,\mathrm{T}_{pe}} \geq 20.0$ ms and $d^{\mathrm{PCA}}_{w,\mathrm{T}_{pe}} < 20.0$ ms (a) and for the pigs with $\mathrm{T}^{\mathrm{PCA}}_{pe} \geq 85.4$ and $\mathrm{T}^{\mathrm{PCA}}_{pe} < 85.4$ (b) at the 5-10 minutes interval from the balloon inflation onset. The p value (Long Rank) is indicated.

TABLE IV: Association of $d^{\mathrm{PCA}}_{w,\mathrm{T}_{pe}}$ and $\mathrm{T}^{\mathrm{PCA}}_{pe}$ with the ocurrence of VF episodes.

	Risk Threshold	**Hazard ratio** (95% CI)	***p*-value**
$d^{\mathrm{PCA}}_{w,\mathrm{T}_{pe}}$	20.0 s	12.5 1.57-99.63	0.017
$\mathrm{T}^{\mathrm{PCA}}_{pe}$	85.4 s	5.5 1.16-26.25	0.032

remaining relatively stable thereafter for the Non-VF group and with a higher rate of increase for the Delayed-VF group. The average time course of the $d^{\mathrm{PCA}}_{w,\mathrm{T}_{pe}}$ index denotes a visibly smoother signal trend than for $\mathrm{T}^{\mathrm{PCA}}_{pe}$ index, implying an improved robustness of $d^{\mathrm{PCA}}_{w,\mathrm{T}_{pe}}$ over $\mathrm{T}^{\mathrm{PCA}}_{pe}$ to quantify ischemia-induced repolarization changes, that could be attributed to a more accurate representation of the underlying physiological changes or a higher measurement stability, or a combination

of both factors.

According to the statistical analysis, $d^{\text{PCA}}_{w,\text{T}_{pe}}$ and $\text{T}^{\text{PCA}}_{pe}$ indices captured changes in the T_{pe} interval, and their magnitudes were statistically different between Non-VF and Delayed-VF groups. The fact that $d^{\text{PCA}}_{w,\text{T}_{pe}}$ and $\text{T}^{\text{PCA}}_{pe}$ indices presented significant intergroup differences from the first interval (0-5 min) suggests that both indices are sensitive enough to capture the ischemic-induced VRD changes as soon as blood supply in the artery coronary is compromised. Furthermore, the p-value of the Mann-Whitney test for mean differences was smaller for $d^{\text{PCA}}_{w,\text{T}_{pe}}$ in the intervals presented in Fig. 5 and Table II, except for a negligible difference in the 5-minutes interval before VF, supporting the hypothesis that $d^{\text{PCA}}_{w,\text{T}_{pe}}$ is a more robust measure of the changes in the T-peak-to-T-end interval than the $\text{T}^{\text{PCA}}_{pe}$ index for arrhythmia prediction. In contrast, $d^{\text{PCA}}_{w,\text{T}}$ increases since the beginning of the exposure to ischaemia and reaches a slightly higher, but not statistically significant, range for the Delayed-VF group than for the Non-VF group at all intervals. The latter confirmed that the first part of the T wave (up to T-peak) negatively influences risk markers and is of no value in discriminating between groups, either because it does not specifically represent ischaemia-induced dispersion of repolarization or because ST-segment depression/elevation masks morphological changes related to arrhythmic risk.

As above-mentioned, $d^{\text{PCA}}_{w,\text{T}_{pe}}$ and $\text{T}^{\text{PCA}}_{pe}$ magnitudes increased significantly for the Delayed-VF group with respect to the Non-VF group, allowing us to evaluate them as VF predictors. Both indices distinguished between groups within the last 5 minutes before VF episode interval, always favoring $d^{\text{PCA}}_{w,\text{T}_{pe}}$. Likewise, and more clinically relevant, $d^{\text{PCA}}_{w,\text{T}_{pe}}$ was also able to discriminate between groups already from the prior interval to the arrhythimic window (5-10 min interval), and even for the earlier 0-5 min interval. The AUC for $d^{\text{PCA}}_{w,\text{T}_{pe}}$ was systematically greater than that of the $\text{T}^{\text{PCA}}_{pe}$ index. In brief, a $d^{\text{PCA}}_{w,\text{T}_{pe}}$ increase beyond the cut-off value of 20.0 ms in the early 5-10 min interval from the occlusion onset predicted impending VF episodes with 90.0% of Se and 75.0% of Sp, while a cut-off value of 85.4 ms for $\text{T}^{\text{PCA}}_{pe}$ index achieved 80.0% of Se and 69.0% of Sp. Moreover, a higher hazard ratio was obtained for $d^{\text{PCA}}_{w,\text{T}_{pe}}$ (12.5) than for $\text{T}^{\text{PCA}}_{pe}$ (5.5) by the Cox regression analysis.

We have analyzed and focused on the Delayed-VF episodes, which are believed to have different underlying mechanisms than the early VF [24], and they typically occur after patient's initial interaction with healthcare professionals. According to speed of infarct progression in pigs, which is approximately 7 times faster with respect to that of the humans [31], the analyzed VF in this study corresponds to the arrhythmias reported in humans after around two hours. Therefore, predicting Delayed-VF does have a potential clinical significance.

C. Limitations

In this experimental study, only LAD occlusions were induced, therefore we were not able to evaluate the behavior of $d^{\text{PCA}}_{w,\text{T}_{pe}}$ with regard to different localization of ischemia, which are known to have also an effect on arrhythmic risk. Another potential issue is the fact that the pigs were anesthetized. Hence, it is crucial to further evaluate the index in high-risk humans population and to exercise caution when extrapolating our findings in pigs to clinical settings.

Other aspect to mention is the need for a T-wave reference when evaluating the risk. This reference, here taken at the first 60 s of baseline stage, may not be available in a clinical setting, requiring alternative ways to obtain it. They could be extracted from prerecorded control ECG recordings, or, when not available, average patterns extracted from large patient libraries, as done in[9].

V. Conclusions

The time-warping-based morphology index, $d^{\text{PCA}}_{w,\text{T}_{pe}}$, restricted from the peak to end of T-wave, captures the changes in ischemia-induced ventricular repolarization dispersion. The dynamic increases of $d^{\text{PCA}}_{w,\text{T}_{pe}}$ magnitude beyond certain thresholds predict VF episodes better than $\text{T}^{\text{PCA}}_{pe}$ as ischemia progresses in a myocardial infarction porcine model and advices further evaluation in a human population.

Acknowledgments

This work was supported by projects PID2019-104881RB-I00, PID2021-128972OA-100 and TED2021-130459B-I00 funded by Spanish Ministry of Science and Innovation (MCIN) and FEDER, and by Gobierno de Aragón to project LMP141-21, and to the Biomedical Signal Interpretation and Computational Simulation (BSICoS) Group T39-23R 2014-2020. JR acknowledges funding from fellowship RYC2021-031413-I from MICIN.

References

[1] A. Alonso *et al.*, "Heart disease and stroke statistics—2021 update," *Circulation*, vol. 2021, no. 143, pp. e00–e00, 2021.

[2] A. Timmis *et al.*, "European society of cardiology: cardiovascular disease statistics 2019," *European heart journal*, vol. 41, no. 1, pp. 12–85, 2020.

[3] T. V. Kenttä *et al.*, "Repolarization heterogeneity measured with T-wave area dispersion in standard 12-lead ECG predicts sudden cardiac death in general population," *Circulation: Arrhythmia and Electrophysiology*, vol. 11, no. 2, p. e005762, 2018.

[4] M. S. Fuller *et al.*, "Estimates of repolarization dispersion from electrocardiographic measurements," *Circulation*, vol. 102, no. 6, pp. 685–691, 2000.

[5] P. Laguna *et al.*, "Techniques for ventricular repolarization instability assessment from the ECG," *Proceedings of the IEEE*, vol. 104, no. 2, 2016.

[6] M. M. Demidova *et al.*, "T wave alternans in experimental myocardial infarction: Time course and predictive value for the assessment of myocardial damage," *Journal of Electrocardiology*, vol. 46, no. 3, pp. 263–269, 2013.

[7] R. L. Verrier *et al.*, "Microvolt T-wave alternans: physiological basis, methods of measurement, and clinical utility—consensus guideline by international society for Holter and noninvasive electrocardiology," *Journal of the American College of Cardiology*, vol. 58, no. 13, pp. 1309–1324, 2011.

[8] J. Ramírez *et al.*, "Variability of ventricular repolarization dispersion quantified by time-warping the morphology of the T-waves," *IEEE Transactions on Biomedical Engineering*, vol. 64, no. 7, pp. 1619–1630, 2016.

[9] J. Ramírez *et al.*, "ECG T-wave morphologic variations predict ventricular arrhythmic risk in low-and moderate-risk populations," *Journal of the American Heart Association*, vol. 11, no. 17, p. e025897, 2022.

[10] G.-X. Yan and C. Antzelevitch, "Cellular basis for the normal T wave and the electrocardiographic manifestations of the long-QT syndrome," *Circulation*, vol. 98, no. 18, pp. 1928–1936, 1998.

[11] C. Antzelevitch *et al.*, "Does Tpeak–Tend provide an index of transmural dispersion of repolarization?," *Heart rhythm*, vol. 4, no. 8, pp. 1114–1116, 2007.

[12] C. Antzelevitch *et al.*, "Tpeak-Tend as a predictor of ventricular arrhythmogenesis," *International Journal of Cardiology*, vol. 249, pp. 75–76, 2017.

[13] T. Opthof *et al.*, "Dispersion of repolarization in canine ventricle and the electrocardiographic T wave: Tp-e interval does not reflect transmural dispersion," *Heart Rhythm*, vol. 4, no. 3, pp. 341–348, 2007.

[14] N. V. Arteyeva *et al.*, "What does the Tpeak-Tend interval reflect? an experimental and model study," *Journal of Electrocardiology*, vol. 46, no. 4, pp. 296–e1, 2013.

[15] K. Takenaka *et al.*, "Exercise stress test amplifies genotype-phenotype correlation in the LQT1 and LQT2 forms of the long-QT syndrome," *Circulation*, vol. 107, no. 6, pp. 838–844, 2003.

[16] C. Patel and C. Antzelevitch, "Cellular basis for arrhythmogenesis in an experimental model of the SQT1 form of the short QT syndrome," *Heart Rhythm*, vol. 5, no. 4, pp. 585–590, 2008.

[17] W. Xianpei *et al.*, "Tpeak-Tend dispersion as a predictor for malignant arrhythmia events in patients with vasospastic angina," *International Journal of Cardiology*, vol. 249, pp. 61–65, 2017.

[18] P. Maury *et al.*, "Increased Tpeak-Tend interval is highly and independently related to arrhythmic events in Brugada syndrome," *Heart Rhythm*, vol. 12, no. 12, pp. 2469–2476, 2015.

[19] J. E. Azarov *et al.*, "Progressive increase of the T peak-T end interval is associated with ischaemia-induced ventricular fibrillation in a porcine myocardial infarction model," *EP Europace*, vol. 20, no. 5, pp. 880–886, 2018.

[20] N. Gómez *et al.*, "Time-warping analysis of the t-wave peak-to-end interval to quantify ventricular repolarization dispersion during ischemia," *IEEE Journal of Biomedical and Health Informatics*, pp. 1–12, 2023.

[21] N. Gómez *et al.*, "Changes in t-peak-to-t-end morphology measured by time-warping are associated with ischemia-induced ventricular fibrillation in a porcine model," in *2023 Computing in Cardiology (CinC)*, vol. 50, pp. 1–4, 2023.

[22] M. M. Demidova *et al.*, "S-segment dynamics during reperfusion period and the size of myocardial injury in experimental myocardial infarction," *Journal of electrocardiology*, vol. 44, no. 1, pp. 74–81, 2011.

[23] E. Kaplinsky *et al.*, "Two periods of early ventricular arrhythmia in the canine acute myocardial infarction model.," *Circulation*, vol. 60, no. 2, pp. 397–403, 1979.

[24] U. Menken *et al.*, "Prophylaxis of ventricular fibrillation after acute experimental coronary occlusion by chronic beta-adrenoceptor blockade with atenolol," *Cardiovascular Research*, vol. 13, no. 10, pp. 588–594, 1979.

[25] J. P. Martínez *et al.*, "A wavelet-based ECG delineator: evaluation on standard databases," *IEEE Transactions on biomedical engineering*, vol. 51, no. 4, pp. 570–581, 2004.

[26] P. Laguna *et al.*, "Automatic detection of wave boundaries in multilead ECG signals: Validation with the CSE database," *Computers and biomedical research*, vol. 27, no. 1, pp. 45–60, 1994.

[27] F. Castells *et al.*, "Principal component analysis in ECG signal processing," *EURASIP Journal on Advances in Signal Processing*, vol. 2007, pp. 1–21, 2007.

[28] S. Palacios *et al.*, "Sudden cardiac death prediction in chronic heart failure patients by periodic repolarization dynamics," in *2020 Computing in Cardiology*, pp. 1–4, IEEE, 2020.

[29] J. D. Tucker, W. Wu, and A. Srivastava, "Generative models for functional data using phase and amplitude separation," *Computational Statistics & Data Analysis*, vol. 61, pp. 50–66, 2013.

[30] D. P. Bertsekas, "Vol. 1 of dynamic programming and optimal control," *Athena scientific Belmont, MA*, 2005.

[31] E. Hedström *et al.*, "Infarct evolution in man studied in patients with first-time coronary occlusion in comparison to different species-implications for assessment of myocardial salvage," *Journal of Cardiovascular Magnetic Resonance*, vol. 11, pp. 1–10, 2009.